Zero-Residual-Energy, Single-Axis Slew of Flexible Spacecraft Using Thrusters: Dynamics Approach

Hari B. Hablani*
Rockwell International, Seal Beach, California 90740

By examining the phase plane response of an elastic mode to a sequence of step torques, the paper first shows that if the half-slew time is an integer times the modal period, a flexible spacecraft can be slewed with zero residual energy in one critical mode. Because this stipulation cannot be met for an arbitrary slew angle and slew acceleration, two intervening pulses of equal width for undamped mode, and of unequal width for damped mode, are shown to be required to achieve two goals at once: 1) slew the spacecraft by the desired angle, and 2) have zero residual energy in a critical elastic mode. Using elementary structural dynamics, easily solvable analytical relationships are developed among the rest-to-rest maneuver angle, slew acceleration, slew time, widths of the intervening pulses, natural frequency of the critical mode, and its damping coefficient. This minimum-time, zero-residual-energy, single-axis slew is illustrated on a spacecraft with two solar arrays. In addition, the assumption of only one elastic mode being critical is carefully examined. To bring cohesion between this work and the works in the past, the place of this contribution is identified. Finally, to bring an *arbitrary* rigid and elastic modal state of a flexible spacecraft to the origin, a conceptual, discrete control scheme using thrusters is suggested.

I. Introduction

THE problem of slewing a rigid spacecraft using thrusters, particularly when this problem is regarded as a branch of mass expulsion spacecraft attitude control discipline, has been investigated to great depths over the last three decades. During the last decade in particular, as the spacecraft have become significantly more flexible with the growing size of the solar arrays, and currently, as the large space structures are becoming a reality, the nonlinear discipline of the reaction jet controllers is becoming ever more important. For rigid spacecraft, the techniques of designing a reaction jet controller that meets performance specifications are well established. In contrast, for flexible spacecraft, the complications in designing such a controller are proportional to the degree of flexibility and to the stringency of the attitude and rate jitter specifications. In an attempt to simplify some of the issues involved, our objective in this paper is to expose fundamental relationships among the rest-to-rest slew angle of the spacecraft, multiple switching times of a slew acceleration profile using on-off thrusters, and the frequency of a critical spacecraft mode having quantifiable structural damping; these relationships arise from the requirement that a critical spacecraft mode must have zero energy at the end of the slew. The approach adopted here is not the widespread modern optimal control approach, with its poignant minimum principle of Pontryagin, the Hamilton-Jacobi equation, the costate equations, and such, because apparently this first-order state space apparatus beclouds the simple responses of a rigid and an elastic mode to a sequence of step torques. To obtain the aforementioned relationships, we will therefore employ elementary structural dynamics.

Brief Review of the Literature

To set apart the contributions of this paper and to interweave the pertinent literature, we give a brief account of significant facets of the problem of slewing a flexible spacecraft comprises and how they have been variously viewed in the past within a broader context of the attitude control of flexible space structures using thrusters. We mention only those contributions that are related to this paper and indicate the punctuated progress that has taken place in this field over the years. To begin with, we observe that, for attitude control or slew maneuver of a rigid spacecraft using thrusters, two of the several classical control policies are minimum time and weighted time fuel,[1] the latter policy capitalizing on the free coasting of the spacecraft toward the desired state, saving fuel thereby at the cost of time. Ideal engineering realizations of these policies for a principal-axis maneuver are diagrammed in Fig. 7.5 and Fig. 8.13 of Ref. 1. D'Amario and Stubbs[2] have designed a variant of the weighted time-fuel control policy for a single-rotation-axis (Euler axis) maneuver even when there exists a strong interaxial coupling arising from the cross products or unequal moments of inertia, or rapid rates. Because of the coupling, the angular acceleration command is adjusted (instead of keeping it constant, as in Ref. 1) so that almost full torque capacity is utilized during the maneuver (except while coasting). To realize this slew, Ref. 2 also provides a block diagram utilizing a gimbal-less advanced inertial reference system for attitude determination. There are several reaction jet controllers for attitude control or slew maneuver that are based on pulse-width modulation, pulse-frequency modulation, or both or on integral pulse frequency modulation; see Farrenkopf et al.,[3] for example. White et al.[4] have proved that these controllers are equivalent to the weighted time-fuel optimal controllers.

The spacecraft of recent times are of course not rigid, and their attitude motion consists of rigid as well as elastic modes. Precise attitude control or slew maneuver, therefore, demands that both sets of modes be controlled. Interestingly, the control of the elastic modes alone using thrusters has been considered in the literature; for example, see Ref. 1, Sec. 7.7, wherein a time-optimal controller has been designed for that purpose. The controller involves a scallop-like switch curve (Fig. 7.42, Ref. 1), with the control torque acting until the modal amplitude is brought down to zero, the jet force changing its sign every half modal period. Suboptimal, that is, simpler switch curves are also considered in Sec. 7.7 of Ref. 1, as is the time-optimal control of a damped oscillator (Sec. 7.8, Ref. 1). These controllers, optimal or suboptimal, however, do not use fuel efficiently because as Refs. 5 and 6 show, the

Received April 30, 1990; revision received Nov. 15, 1990; accepted for publication Feb. 12, 1991.

*Engineering Specialist, Guidance and Control Group, Space Systems Division. Senior Member AIAA.

modal energy is extracted most efficiently if the jets are fired around the peak modal rates and not all the way as in Ref. 1. With this in mind, de Oliveira e Souza[7] has given an exact, weighted time-fuel optimal controller for undamped harmonic oscillators, according to which the thrusters are indeed fired around peak modal rates. Reference 5, using an adaptive bandpass filter, gives a scheme for estimating when the peak rate of a certain mode will occur. To bring an arbitrary state of the spacecraft (that is, arbitrary rigid attitude and rate and arbitrary deformed modal state, within the assumptions of linear elasticity) to the origin, the optimal controller of Ref. 7 for an elastic mode must be implemented along with a weighted time-fuel optimal controller for a rigid mode based on the design in Ref. 6. However, insofar as these two optimal controllers are designed independently, the spacecraft's state chatters near the origin.[6,7] This indicates the need for a well-coordinated thruster controller that controls a rigid mode and, simultaneously, suppresses a critical elastic mode as well. Further discussion along this line is deferred until Sec. V.

The problem of the rest-to-rest slew with zero residual energy in a critical elastic mode (the theme of this paper) is simpler than the problem of bringing an arbitrary state of a flexible spacecraft to the origin (Vander Velde and He[6] considered the latter problem). Although Skaar et al.[8] do not state it, they have considered a weighted time-fuel optimal controller for the former problem using the principles of dynamics, not optimal control. The motivation behind their introducing a coasting phase in the slew maneuver is to acquire freedom in the termination of the slew maneuver so that the termination occurs not only when the spacecraft has slewed by the desired angle, but also when the total deformational energy in six spacecraft modes is zero as well. Later on, Rajan[9] showed that the minimum-time control for the rest-to-rest slew with zero residual energy in one critical mode at the end of the slew consists of three switches in the torque profile around the half-slew time. Singh et al.[10] have obtained, also using time-optimal control theory, a general result that the energy in n undamped spacecraft modes at the end of the slew can be zeroed with $(2n + 1)$ switches in the torque profile around the half-slew time. References 8–10, nevertheless, do not determine a parametric relationship of the sort mentioned above in the first paragraph.

Apart from the time-optimal or time-fuel optimal studies, there have been a significant number of other studies as well on the topic under consideration. A few important citations are the book by Junkins and Turner,[11] early theoretical as well as experimental studies by Breakwell[12] and Juang et al.[13] based on linear optimal control theory and linear actuators, a recent study by Junkins et al.[14] that uses a combination of shaped torque profile for near-minimum-time maneuver and proportional-plus-derivative-plus-acceleration controller, and a related prior study by Byers et al.[15] using tanh function as a smooth approximation to the discontinuous sign function. But these studies employ linear actuators, which are not within the intended scope of the present paper.

Modeling Issues of the Slew Maneuver of Flexible Spacecraft

In view of the several complex math models extant in the literature dealing with the topic at hand, there are several issues that should be addressed so that we might develop a model that is realistic and yet amenable to analysis and suits our objective. First, the interaxial coupling is ignored here because only single-axis slew maneuver about a principal axis is of concern. The angular rates about the other two axes, if not zero, are restricted to be so small that the nonlinear term in the Euler equation about the slew-axis is at least an order of magnitude smaller than, and so negligible compared with, the slew torque. Parenthetically, note that this assumption is not made in Ref. 2. Second, for single-axis large-angle maneuver of a flexible spacecraft, Junkins and Turner[11] developed Eqs. (9–13) and Eqs. (9–14) that include nonlinear terms arising from 1) foreshortening effect of the deforming elastic appendage, and 2) rotational stiffening effect of the centrifugal force due to the slew rates. These nonlinear terms may be important in some situations, but in the rest-to-rest slew example, case 5 in Sec. 9.6 of Ref. 11, they are found to be negligible compared to the linear terms; even in the spin-up and spin-reversal maneuvers, cases 8 and 11 in the same reference, the nonlinear effects remain insignificant. This is expected since a slew is a transient phenomenon—the slew rate profile begins and ends with zero and hovers near the maximum rate briefly. The centrifugal force is therefore essentially ephemeral. Besides, this force is attenuated furthermore by the frequency response characteristics of the elastic modes. Also, the spin maneuvers of a flexible spacecraft are typically slow, unlike those of the wings of a rotary wing aircraft where the aforementioned nonlinear effects are distinctly important. Thus, all evidence indicates that it is safe to ignore these nonlinear terms, and hence we do so in the following analysis.

The third modeling aspect to be addressed is the appendage modes vs the vehicle modes. For this, we observe that the spacecraft motion equations based on appendage modes (also called hybrid coordinate approach) exhibit linear coupling between spacecraft attitude angle and elastic vibrations [see Eqs. (6) and (7) of Ref. 10, or more streamlined Eqs. (13) of Ref. 16]. Since this coupling hampers the analysis, even those studies that do begin with appendage modes soon transform the coupled equations to the uncoupled ones that represent system modes or vehicle modes, comprising a rigid mode and elastic modes. It is nontrivial to insure that the system modes thus calculated do not suffer from the errors due to the truncation of the appendage modes; see Ref. 17 for modal identity checks for that purpose. Skaar et al.[8] performed the aforementioned transformation perhaps unwittingly by defining what they called an "average" angular position θ_A [Eq. (4), Ref. 8], which is, in fact, a rigid mode angle, and by writing the impulse response, Eq. (25), Ref. 8, as a sum of the rigid mode response and infinite elastic modal responses; compare Eq. (25), Ref. 8, with Eq. (17), Ref. 16. Although Singh et al.[10] do not state it, they too define a variable denoted x_1 in their Eq. (10) that is a rigid mode angle. Since in the literature there are in-depth, exhaustive studies that compare appendage mode and vehicle mode formulations (see Refs. 16–18), we shall be content with stating that, because the vehicle mode formulation affords simple, linear, uncoupled, amenable equations of motion, we will use that here, following Refs. 6, 9, and 12.

We finally address the question of how many modes to retain in the analysis and simulation. For this, let Φ_μ be the contribution of a vehicle mode μ to the spacecraft attitude; that is, if $\eta_\mu(t)$ is the μth modal coordinate (t = time), then $\Phi_\mu \eta_\mu(t)$ is the spacecraft attitude due to this mode [see the modal expansion Eq. (69), Ref. 18]. When a step torque T_{mx} is applied to slew the spacecraft, the maximum contribution of the undamped mode μ to the spacecraft attitude is known to be $2\Phi_\mu^2 T_{mx}/\omega_\mu^2$ (ω_μ = the frequency of the mode μ), which may be rewritten as $2\Phi_\mu^2 I\alpha_{mx}/\omega_\mu^2$, where I equals the spacecraft's moment of inertia about the slew axis, and α_{mx} is the slew acceleration. On the other hand, with the aid of the identity (T) and the second equation of Eqs. (59), Ref. 18, it can be shown that for single axis the coefficients Φ_μ ($\mu = 1, 2, \ldots$) obey the identity

$$I\sum_{\mu=1}^{\infty}\Phi_\mu^2 = I_f/I_r,\ (I = I_f + Ir) \tag{1}$$

where I_f and I_r are, respectively, the principal, central moment of inertia of the flexible and the rigid portions of the vehicle about the slew axis. Clearly, for a constant I, as the vehicle becomes more flexible (that is, as I_f goes up and I_r down), the coefficients Φ_μ ($\mu = 1, 2, \ldots$) become larger, and as long as $I_r \neq 0$, the coefficients Φ_μ constitute a convergent series; that is, sooner or later they begin to diminish and the coefficients Φ_μ^2/ω_μ^2 diminish even more rapidly with μ. Next, we observe that in the case of a real slew maneuver the structural engineer

would recommend keeping the structure surface—if it is two dimensional—in the slew plane so that the slew induces in-plane vibrations, for which Φ_μ are smaller and ω_μ higher than those for the transverse bending vibrations. These arguments suggest that for the in-plane vibrations and for $I_f/I_r < 1$, we may have $\Phi_2^2/\omega_2^2 \ll \Phi_1^2/\omega_1^2$, implying that, under stated circumstances, the analysis may be fruitfully conducted with one mode only; the accuracy of this assumption can, of course, be checked by retaining more than one mode in the simulation. This is precisely the course we have followed in this study.

Organization of the Paper

In Sec. II, we closely examine the phase-plane response of an undamped structural mode excited by a sequence of step torques used for slewing the spacecraft. Calling upon the fundamentals of structural dynamics, an insight is thereby gained into the mechanics of this excitation, from which emerges a torque profile with two equal, narrow, compensating pulses around the half-slew time (identical to those in Refs. 9 and 10) fulfilling two requirements at once: it slews the spacecraft by the desired angle and it zeroes out the energy in an undamped, critical flexible mode at the end of the slew. For damped modes, in Sec. III, we develop analytical relationships among the widths of two unequal intervening pulses, slew time, maneuver angle, critical modal frequency, and structural damping, meeting the aforementioned two requirements. Numerical results illustrating the theory are discussed in Sec. IV. In Sec. V, we give a conceptual scheme for controlling a flexible spacecraft from an arbitrary state—arbitrary attitude and arbitrary deformation in one mode and their arbitrary rates—with reaction jets, firing periodically at modal frequency with some optimum pulse width. Section VI concludes the paper.

II. Phase-Plane Responses of an Undamped Mode to Minimum-Time Slew Torque Profiles

Let $\Theta(t)$ denote the rigid mode attitude of the spacecraft about the slew axis; Θ_i and Θ_f denote the initial and the final rigid angles of the spacecraft. Then, if t_f is the minimum time required for slewing the spacecraft from Θ_i to Θ_f, it is known that

$$t_f = 2[(\Theta_f - \Theta_i)I/T_{mx}]^{1/2} \tag{2}$$

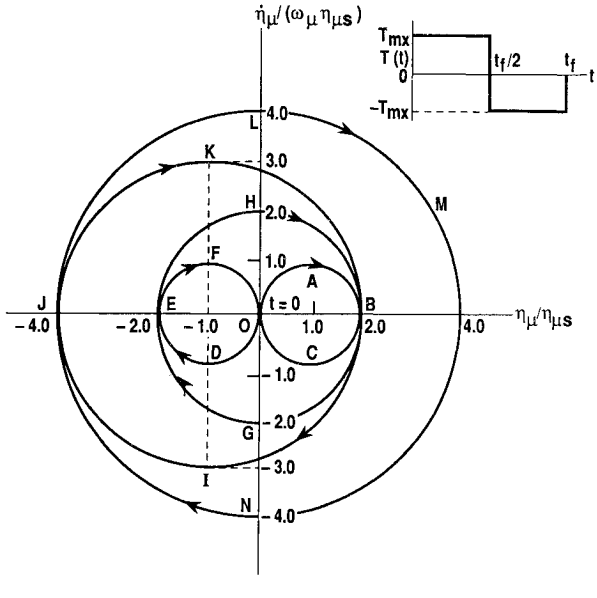

Fig. 1 Dependence of modal excitation on the switching times of a bang-bang torque profile.

This equation is obtained by solving the following rigid mode equation that governs the single-axis, time-optimal slew maneuver of a spacecraft about a central, principal axis:

$$I\ddot\Theta = \begin{cases} T_{mx} & 0 \le t \le t_f/2 \\ -T_{mx} & t_f/2 \le t \le t_f \\ 0 & t_f \le t \end{cases} \tag{3}$$

To write the equation of motion of a vehicle elastic mode μ ($\mu = 1, 2, \ldots, \infty$), let F_{mx} be the jet force associated with the torque T_{mx}, and let $\chi_{\mu J}$ denote the μth translational modal coefficient at the jet location. If the jet resides in the rigid central body, then, for the antisymmetric modes, $\chi_{\mu J}$ is related to Φ_μ, defined earlier, as follows:

$$\chi_{\mu J}F_{mx} = \Phi_\mu T_{mx} \tag{4}$$

wherein the jet moment arm is implicit. Equation (4), however, is not valid if the jet is located on the deformable structure because then $\chi_{\mu J}$ is not only due to Φ_μ but there is an additional, local deformation as well, contributing to $\chi_{\mu J}$. Moreover, although Eq. (4) is written for only one jet acting on the spacecraft, an equivalent $\chi_{\mu J}$ can be developed if more than one jet, perhaps inclined to the principal axes, are used in concert to produce T_{mx}. In any event, the μth vehicle modal coordinate $\eta_\mu(t)$ during and after the slew maneuver is governed by

$$\ddot\eta_\mu + 2\zeta_\mu\omega_\mu\dot\eta_\mu + \omega_\mu^2\eta_\mu = \begin{cases} \chi_{\mu J}F_{mx} & 0 \le t \le t_f/2 \\ -\chi_{\mu J}F_{mx} & t_f/2 \le t \le t_f \\ 0 & t_f \le t \end{cases} \qquad (\mu = 1, 2, \ldots) \tag{5}$$

where ζ_μ is an equivalent viscous damping coefficient of μth mode, and $(\dot{}) = \mathrm{d}(\ )/\mathrm{d}t$. In this section, ζ_μ equals zero. The total spacecraft attitude $\theta(t)$, meanwhile, is given by

$$\theta(t) = \Theta(t) + \sum_{\mu=1}^{\infty} \Phi_\mu\eta_\mu(t) \tag{6}$$

Unbeguiled by the simplicity of the modal equations (3) and (5), these are indeed time-honored, classic equations; for one thing, they are akin to Eqs. (3.204) of 1955 vintage[19] for studying the deformable airplane dynamics. For the other, they are equivalent, after reconciling the notations, to the state space models, Eqs. (14-17) of Ref. 10, and Eqs. (17) and (18) of Ref. 6, except for some unimportant differences regarding the number and the location of the jets.

To probe the mechanics of the excitation of an elastic mode as the slew torque $T(t)$ performs its bang-bang profile, we set $\zeta_\mu = 0$ in Eq. (5), solve it for $0 \le t < t_f/2$ with the initial conditions $\dot\eta_\mu(0) = 0 = \eta_\mu(0)$, and obtain the well-known relationships

$$\eta_\mu(t) = \eta_{\mu s}(1 - \cos\omega_\mu t) \tag{7a}$$

$$\dot\eta_\mu(t) = \omega_\mu\eta_{\mu s}\sin\omega_\mu t \qquad 0 \le t < t_f/2 \tag{7b}$$

where the static deformation $\eta_{\mu s}$ is defined as

$$\eta_{\mu s} = \chi_{\mu J}F_{mx}/\omega_\mu^2 = \Phi_\mu T_{mx}/\omega_\mu^2 \tag{7c}$$

From Eq. (7a), the maximum value of $\eta_\mu(t)$ is $2\eta_{\mu s}$, so the maximum spacecraft angle due to the mode μ will be $2\eta_{\mu s}\,\Phi_\mu$ or $2\Phi_\mu^2 T_{mx}/\omega_\mu^2$; it is this quantity that was used earlier in the subsection Modeling Issues. In the normalized phase plane, $\dot\eta_\mu/(\omega_\mu\eta_{\mu s})$ vs $\eta_\mu/\eta_{\mu s}$, Fig. 1, Eqs. (7a) and (7b) appear as the circle 0ABC0, where we observe that $0 \le \eta_\mu(t) \le 2\eta_{\mu s}$, and $-\omega_\mu\eta_{\mu s} \le \dot\eta_\mu(t) \le \omega_\mu\eta_{\mu s}$. When $t = n\tau_\mu$ ($\tau_\mu = 2\pi/\omega_\mu$, the period

of the mode μ, and $n = 1, 2, 3, \ldots$), both η_μ and $\dot{\eta}_\mu$ are zero; that is, the energy of the mode at $t = n\tau_\mu$ is zero. Therefore, if the step torque T_{mx} and the concomitant step force F_{mx} are removed at $t = n\tau_\mu$ (at the origin 0 in Fig. 1), the mode μ (only one mode, not all) will not vibrate thereafter. On the other hand, if the torque T_{mx} switches to $-T_{mx}$ at $t = n\tau_\mu = t_f/2$ and thereby the product $\chi_{\mu J}F_{mx}$ switches to $-\chi_{\mu J}F_{mx}$, then the mode will begin to vibrate in accordance with

$$\eta_\mu(t) = -\eta_{\mu s}(1 - \cos\omega_\mu t), \qquad \dot{\eta}_\mu(t) = -\omega_\mu \eta_{\mu s} \sin\omega_\mu t$$

$$t \geq n\tau_\mu = t_f/2 \tag{8}$$

which is shown as the circle 0DEF0 in Fig. 1. Comparing Eqs. (8) with Eqs. (7a) and (7b), we deduce that under these especial circumstances, $\eta_\mu(t)$ vs t is antisymmetric with respect to the vertical line $t = n\tau_\mu$, and $\dot{\eta}_\mu(t)$ vs t symmetric. Once again, if $-T_{mx}$ is now removed at 0, after $t = (n + m)\tau_\mu$, where m is another integer, not necessarily different from n, the mode μ (only one mode as before, not all) will cease to oscillate, as intended.

In contrast with this zero-residual-energy aspect, there exists a worst-residual-energy aspect too. From Eqs. (7a) and (7b) and from Fig. 1, we gather that if T_{mx} is terminated at $t = (n - \frac{1}{2})\tau_\mu$, that is, at the point B in Fig. 1 where $\eta_\mu = 2\eta_{\mu s}$ and $\dot{\eta}_\mu = 0$, then because of the stored energy $E_\mu = \frac{1}{2}\omega_\mu^2(2\eta_{\mu s})^2$, the mode will oscillate with an amplitude of $2\eta_{\mu s}$ and zero average (the circle BGEHB, Fig. 1). On the other hand, if, instead of becoming zero, T_{mx} switches instantly to $-T_{mx}$ and the product $\chi_{\mu J}F_{mx}$ to $-\chi_{\mu J}F_{mx}$, the static deformation will also switch from $\eta_{\mu s}$ to $-\eta_{\mu s}$, and from this new static state [the point $(-1, 0)$ in Fig. 1] the modal coordinate η_μ at B is 3 $\eta_{\mu s}$ away. Therefore, η_μ will now execute the circle BIJKB, oscillating between $-4\eta_{\mu s}$ and $2\eta_{\mu s}$, with the average $-\eta_{\mu s}$. The circle BIJKB is described by

$$\eta_\mu(t) = -\eta_{\mu s}(1 + 3\cos\omega_\mu t), \qquad \dot{\eta}_\mu(t) = 3\eta_{\mu s}\omega_\mu \sin\omega_\mu t$$

$$t \geq (n - \tfrac{1}{2})\tau_\mu = t_f/2 \tag{9}$$

Compared to the circle 0DEF0 of radius unity, the cocentric circle BIJKB is of radius 3, although they both have the same static deformation [the center $(-1, 0)$]. The oscillations will worsen yet if the torque $-T_{mx}$ is now terminated at the point J in Fig. 1, because there $\eta_\mu = -4\eta_{\mu s}$ and $\dot{\eta}_\mu = 0$, and therefore the mode will oscillate with $4\eta_{\mu s}$ amplitude and zero average (the circle JLMNJ). On the other hand, if $-T_{mx}$ is terminated at B, then the mode will oscillate thereafter with $2\eta_{\mu s}$ amplitude and zero average (the circle BGEHB).

To elucidate the preceding discussion further, we examine the energy E_μ of the μth mode:

$$E_\mu = (\dot{\eta}_\mu^2 + \omega_\mu^2\eta_\mu^2)/2 \tag{10}$$

Taking its derivative and utilizing Eqs. (5) (ζ_μ still zero), we obtain

$$\dot{E}_\mu = \begin{cases} \dot{\eta}_\mu \chi_{\mu J} F_{mx} & 0 \leq t \leq t_f/2 \quad (11a) \\ -\dot{\eta}_\mu \chi_{\mu J} F_{mx} & t_f/2 \leq t \leq t_f \quad (11b) \\ 0 & t_f \leq t \quad (11c) \end{cases}$$

Solving Eq. (11a) and assuming that $\eta_\mu(0) \neq 0$ for generality, we arrive at

$$E_\mu(t) - E_\mu(0) = \chi_{\mu J}F_{mx}[\eta_\mu(t) - \eta_\mu(0)], \qquad 0 \leq t \leq t_f/2 \tag{12}$$

If the force F_{mx} acts for a complete number of oscillations (that is, $n\tau_\mu$ period), then $\eta_\mu(n\tau_\mu) = \eta_\mu(0)$ and so, according to Eq. (12), the energy input to the mode will be zero. On the other hand, if F_{mx} acts for $(n - \frac{1}{2})\tau_\mu$ s, then, because according to Eq. (7a) and Eq. (7b) [wherein $\eta_\mu(0) = 0 = \dot{\eta}_\mu(0)$] $\eta_\mu = 2\eta_{\mu s}$ at $t = (n - \frac{1}{2})\tau_\mu$, the energy input to the mode becomes

$$E_\mu = 2\chi_{\mu J}F_{mx}\eta_{\mu s} = 2\eta_{\mu s}^2\omega_\mu^2 = \tfrac{1}{2}(2\eta_{\mu s})^2\omega_\mu^2 \qquad \text{at } t = (n - \tfrac{1}{2})\tau_\mu \tag{13}$$

This energy input is the cause of the phase-plane motion BGEHB in Fig. 1 when F_{mx} is removed after $t = (n - \frac{1}{2})\tau_\mu$. The resemblance of this discussion of energy with the previous discussion of amplitude is now apparent.

The preceding observations bring forth the fact that the bang-bang torque profile does not always lead to excessive residual modal energy. Indeed, for a spacecraft in which only one low-frequency mode is particularly excitable whereas others are high-frequency modes, if the half-slew time is an integer times the period of that particular mode, then, as we saw earlier, the residual energy in that mode after the slew is zero. Such benevolent circumstances are of course rare; the half-slew time dictated by the maneuver requirement will usually conflict with the zero-residual-energy requirement, $t_f/2 = n\tau_\mu$ ($n = 1, 2, 3, \ldots$), for a low-frequency mode. Thus, the need for freeing the half-slew time is evident.

In the preceding zero-residual-modal energy example, we found that $\eta_\mu(t)$ vs t is antisymmetric about $t = t_f/2$ and $\dot{\eta}_\mu(t)$ vs t symmetric. Clearly, $\ddot{\eta}_\mu(t)$ will be antisymmetric, as will the bang-bang torque profile about $t = t_f/2$. Now, an unthrottleable reaction jet control system can produce only $\pm F_{mx}$ force, so the changes that may be introduced in the rigid bang-bang torque profile to free $t_f/2$ must be $\pm T_{mx}$ antisymmetric pulses about the new $t_f/2$ (new because these pulses will alter the original t_f). Also, if we desire only one mode to have zero energy at the end of the slew, the half-slew time should be given only one-parameter freedom. This heuristic argument leads to an antisymmetric torque profile shown in Fig. 2 that has a free parameter σ to adjust t_f and has two narrow pulses each of width $\sigma t_f/2$ around $t_f/2$. Of course, now the slew time t_f is not governed by Eq. (2); a new equation must be developed instead. Not surprisingly, Singh et al.[10] arrived at the same torque profile by applying Pontryagin's minimum principle. As the number of the modes that must have zero residual energy increases, an equal number of free parameters governing the width of the antisymmetric pulses (two per mode) around half-slew time are introduced; see Singh et al.[10] for illustrations.

III. Zero-Residual-Energy Bang-Bang Torque Profile for Damped Space Structures

The antisymmetric equal width intervening torque pulses shown in Fig. 2 for structures with no damping foreshadow unequal pulses for structures with damping. In the remainder of the paper we will show this to be true. A torque profile with unequal pulses around $t_f/2$ is shown in Fig. 3a where the torque changes its signs at t_1, t_2, and t_3 in order for one mode

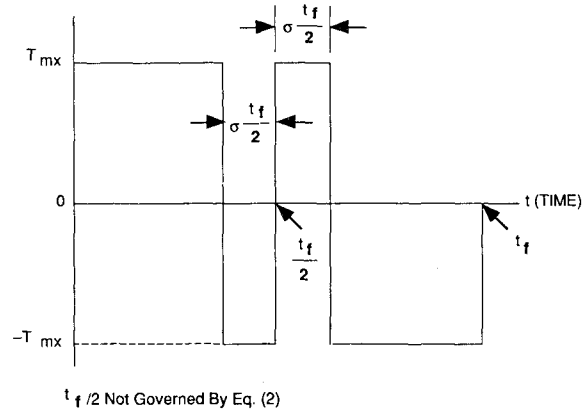

Fig. 2 Bang-bang torque profile with one free parameter for zero residual energy in one undamped flexible mode.

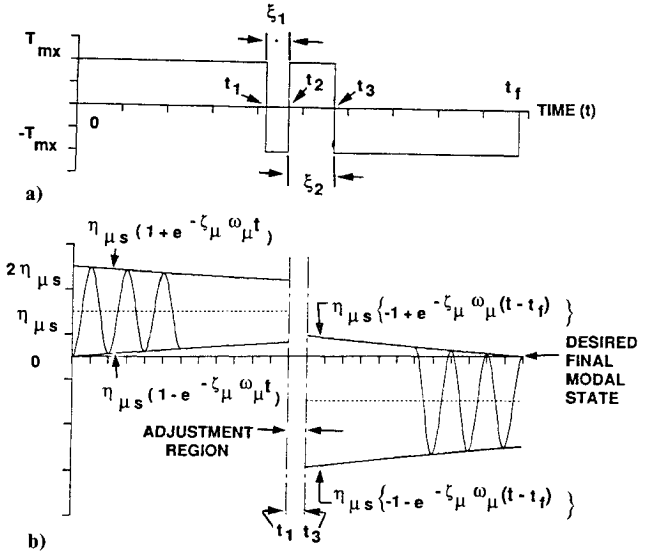

Fig. 3 Zero-residual-energy, minimum-time slew of a flexible space structure with damping: a) torque profile, and b) amplitude envelopes of a modal coordinate whose energy at the end of the slew is zero.

to have zero energy at the end of the slew. We will first explain heuristically how the energy in a mode with damping could be brought off to zero when the slew ends. The initial step torque T_{mx} for $0 \le t \le t_1$ will excite a damped modal coordinate η_μ shown in Fig. 3b. The initial amplitude $\eta_{\mu s}$ of the modal oscillations about the static deformation, also $\eta_{\mu s}$, will decay within the two amplitude envelopes shown in Fig. 3b. At $t = t_1$, the amplitude of the oscillation around the static $\eta_{\mu s}$ will be $\eta_{\mu s}e^{-\zeta_\mu \omega_\mu t_1}$; in contrast to the earlier undamped case, not once is the energy of this mode zero during the interval $0 < t \le t_1$ (because for that to happen both η_μ and $\dot{\eta}_\mu$ must be zero simultaneously). This indicates that, unlike the undamped case, there is no way to terminate T_{mx} at a special moment to have zero residual energy in a critical mode. For the slew to be completed, T_{mx} is not terminated, of course, but reversed to $-T_{mx}$ for which the static deformation is $-\eta_{\mu s}$. Moreover, to satisfy the requirement of zero modal energy at $t = t_f$, the oscillation of the mode at $t = t_f$ must have the amplitude $\eta_{\mu s}$ and such phase that this dynamic amplitude just overcomes the static deformation, and the desired conditions $\eta_\mu(t_f) = 0 = \dot{\eta}_\mu(t_f)$ are acquired. Working backward from t_f (reminiscent of optimal control), then, the amplitude envelopes for $t_3 \le t \le t_f$ will be those shown in Fig. 3b, wherein we observe that the amplitude of the oscillation at t_3 over and above the static deformation $-\eta_{\mu s}$ is $\eta_{\mu s}e^{+\zeta_\mu \omega_\mu (t_f - t_3)}$ which is greater than $\eta_{\mu s}$, implying that extra energy must be added to the structure during $t_1 \le t \le t_3$ to compensate for the energy dissipation during the slew and to acquire the desired dynamic amplitude $\eta_{\mu s}$ at $t = t_f$. The precise determination of the three switching instants t_1, t_2, t_3 and the slew time t_f is examined next.

Determination of Intervening Pulse Widths and Slew Time

The following analysis is for a single axis rest-to-rest slew, that is,

$$\Theta(0) = \Theta_i,\ \dot{\Theta}(0) = 0,\ \Theta(t_f) = \Theta_f,\ \dot{\Theta}(t_f) = 0$$

$$\eta_\mu(0) = 0 = \dot{\eta}_\mu(0), \qquad (\mu = 1, 2, \ldots) \tag{14a}$$

with zero residual energy in only one μth elastic mode:

$$\eta_\mu(t_f) = 0 = \dot{\eta}_\mu(t_f) \tag{14b}$$

For the torque profile shown in Fig. 3a, the widths of the two intervening pulses are

$$\xi_1 \triangleq \sigma_1 t_f/2, \qquad \xi_2 \triangleq \sigma_2 t_f/2 \tag{15}$$

In Fig. 3 and in the following analysis, although $T_{mx} > 0$, the slew requirements may dictate $T_{mx} < 0$, and then $-T_{mx}$ will be > 0; the same applies to $\eta_{\mu s}$. Moreover, the right sides of Eqs. (3) and (5), which pertain to the conventional bang-bang torque profile, are altered to suit the torque profile in Fig. 3a. Therefore, we have

$$I\ddot{\Theta} = \begin{cases} T_{mx} & 0 \le t \le t_1,\ t_2 \le t \le t_3 \\ -T_{mx} & t_1 \le t \le t_2,\ t_3 \le t \le t_f \\ 0 & t_f \le t \end{cases} \tag{16a}$$

$$\ddot{\eta}_\mu + 2\zeta_\mu \omega_\mu \dot{\eta}_\mu + \omega_\mu^2 \eta_\mu = \begin{cases} \chi_{\mu J} F_{mx} & 0 \le t \le t_1,\ t_2 \le t \le t_3 \\ -\chi_{\mu J} F_{mx} & t_1 \le t \le t_2,\ t_3 \le t \le t_f \\ 0 & t_f \le t \end{cases} \tag{16b}$$

To satisfy the requirement of zero slew rate at $t = t_f$, the solution of Eqs. (16a) yields

$$t_1 = t_f/2 - \xi_2, \qquad t_3 = t_f/2 + \xi_1 \tag{17a,b}$$

Next, to satisfy the requirement of slewing the spacecraft by $(\Theta_f - \Theta_i)$ in the duration t_f, Eqs. (16a) lead to

$$\Theta_f - \Theta_i = \alpha_{mx}(t_f/2)^2(1 - 2\sigma_1\sigma_2) \tag{17c}$$

where recall that α_{mx} is the spacecraft's angular acceleration during $0 \le t \le t_1$ and $t_2 \le t \le t_3$. While solving Eqs. (16b), we assume that the damping coefficient ζ_μ is so small that the damped frequency $\omega_{\mu d} \triangleq \omega_\mu \sqrt{1 - \zeta_\mu^2}$ is the same as the undamped frequency ω_μ, and in the response equation the terms multiplied with ζ_μ are negligible compared to those that are not multiplied with ζ_μ. These two safe assumptions allow us to write the solution of the first of Eqs. (16b) with the initial conditions $\eta_\mu(0) = 0 = \dot{\eta}_\mu(0)$ quite simply as

$$\left.\begin{aligned} \eta_\mu(t) &= \eta_{\mu s}(1 - e^{-\zeta_\mu \omega_\mu t}\cos\omega_\mu t) \\ \dot{\eta}_\mu(t) &= \omega_\mu \eta_{\mu s} e^{-\zeta_\mu \omega_\mu t}\sin\omega_\mu t \end{aligned}\right\} \quad 0 \le t \le t_1 \tag{18}$$

The modal state at $t = t_1$ is of special interest, so we introduce the notations

$$c_1 \triangleq \cos\omega_\mu t_1, \qquad s_1 \triangleq \sin\omega_\mu t_1, \qquad e_1 \triangleq e^{-\zeta_\mu \omega_\mu t_1} \tag{19}$$

With the aid of Eqs. (18) and the definitions (19) we obtain, at $t = t_1$,

$$\eta_{\mu 1} \triangleq \eta_\mu(t_1) = \eta_{\mu s}(1 - e_1 c_1), \qquad \dot{\eta}_{\mu 1} \triangleq \dot{\eta}_\mu(t_1) = \omega_\mu \eta_{\mu s} e_1 s_1 \tag{20}$$

Usually the duration $(t_3 - t_1)$ is less than one modal period τ_μ (see Rajan[9] and Singh et al.[10]) for damping to be influential on the modal dynamics, so the damping coefficient ζ_μ will be ignored in this duration. Starting with the initial conditions $\eta_{\mu 1}$, $\dot{\eta}_{\mu 1}$ given by Eqs. (20), the solution of Eq. (16b) in the range $t_1 \le t \le t_2$ yields this modal state at $t = t_2$:

$$\eta_{\mu 2} \triangleq \eta_\mu(t_2) = \eta_{\mu s}(2\cos\omega_\mu \xi_1 - e_1\cos\omega_\mu t_2 - 1)$$

$$\dot{\eta}_{\mu 2} \triangleq \dot{\eta}_\mu(t_2) = \omega_\mu \eta_{\mu s}(-2\sin\omega_\mu \xi_1 + e_1 \sin\omega_\mu t_2) \tag{21}$$

Likewise, starting with the initial conditions (21), the modal state at $t = t_3$ is found to be

$$\eta_{\mu 3} \triangleq \eta_\mu(t_3) = \eta_{\mu s}[2\cos\omega_\mu(\xi_1 + \xi_2) - e_1\cos\omega_\mu t_3 - 2\cos\omega_\mu \xi_2 + 1]$$

$$\dot{\eta}_{\mu 3} \triangleq \dot{\eta}_\mu(t_3) = \omega_\mu \eta_{\mu s}[-2\sin\omega_\mu(\xi_1 + \xi_2) + e_1 \sin\omega_\mu t_3 + 2\sin\omega_\mu \xi_2] \tag{22}$$

Now consider the range $t_3 \le t \le t_f$ in which the damping is of course important. Also, insofar as damping is concerned, it is safe to assume that

$$e^{-\zeta_\mu \omega_\mu t_1} \simeq e^{-\zeta_\mu \omega_\mu t_f/2}, \qquad e^{-\zeta_\mu \omega_\mu (t-t_3)} \simeq e^{-\zeta_\mu \omega_\mu (t-t_f/2)} \tag{23}$$

With this simplification and those stated just before deriving the modal response (18), the modal state $\eta_\mu(t)$ and $\dot{\eta}_\mu(t)$ during $t_3 \le t \le t_f$ is determined by integrating Eq. (16b) with the applicable right side and by using the state (22) as the initial conditions. On this modal response we impose the zero residual energy requirement, Eq. (14b). The following two conditions then emerge:

$$2\sqrt{e_f}[\cos\omega_\mu(t_f/2 + \xi_2) - \cos\omega_\mu(t_f/2 + \xi_2 - \xi_1) + \cos\omega_\mu(t_f/2 - \xi_1)] - e_f \cos\omega_\mu t_f = 1 \tag{24a}$$

$$2\sqrt{e_f}[-\sin\omega_\mu(t_f/2 + \xi_2) + \sin\omega_\mu(t_f/2 + \xi_2 - \xi_1) - \sin\omega_\mu(t_f/2 - \xi_1)] + e_f \sin\omega_\mu t_f = 0 \tag{24b}$$

where Eqs. (17) have been called upon, and

$$e_f \triangleq e^{-\zeta_\mu \omega_\mu t_f}, \qquad \sqrt{e_f} = e^{-\zeta_\mu \omega_\mu t_f/2} \simeq e_1 \tag{25}$$

The condition (24a) insures that the dynamic amplitude $\eta_{\mu s}$ just overcomes the static deformation $-\eta_{\mu s}$ so that $\eta_\mu(t_f)$ is zero, and the condition (24b) guarantees that the modal rate just at that instant is zero as well; consequently, as $-F_{mx}$ turns off at $t = t_f$, the static deformation $-\eta_{\mu s}$ disappears and the structure carries over for all $t > t_f$ its momentary motionless state at $t = t_f$, as desired.

To evaluate the unknowns ξ_1, ξ_2, and t_f, the in-quadrature conditions (24) must be simplified by separating t_f from ξ_1 and ξ_2. For this, we multiply Eq. (24b) with $j(j^2 = -1)$, add it to (and the next time subtract it from) Eq. (24a), and divide throughout by $\sqrt{e_f}\, e^{-j\omega_\mu t_f/2}$. For compactness, we introduce the notations

$$c \triangleq \cos(\omega_\mu t_f/2), \qquad s \triangleq \sin(\omega_\mu t_f/2)$$
$$ch \triangleq \cosh(\zeta_\mu \omega_\mu t_f/2), \qquad sh \triangleq \sinh(\zeta_\mu \omega_\mu t_f/2) \tag{26}$$

The preceding manipulations then lead to a pair of complex equations:

$$e^{-j\omega_\mu \xi_2} - e^{+j\omega_\mu(\xi_1 - \xi_2)} + e^{j\omega_\mu \xi_1} = c \cdot ch + js \cdot sh \tag{27a}$$

$$e^{j\omega_\mu \xi_2} - e^{-j\omega_\mu(\xi_1 - \xi_2)} + e^{-j\omega_\mu \xi_1} = c \cdot ch - js \cdot sh \tag{27b}$$

where now ξ_1 and ξ_2 are on the left sides and t_f on the right. Next, to separate ξ_1 from ξ_2, we determine $e^{j\omega_\mu \xi_1}$ from Eq. (27a) and $e^{-j\omega_\mu \xi_1}$ from Eq. (27b) in terms of ξ_2 and t_f, multiply the two together, and with additional algebra arrive at an exclusive, real relationship between ξ_2 and the half-slew time $t_f/2$:

$$(c \cdot ch - 1)\cos\omega_\mu \xi_2 - s \cdot sh \sin\omega_\mu \xi_2 = (sh^2 - s^2)/2 \tag{28a}$$

Analogously, we obtain a relationship between ξ_1 and $t_f/2$ also:

$$(c \cdot ch - 1)\cos\omega_\mu \xi_1 + s \cdot sh \sin\omega_\mu \xi_1 = (sh^2 - s^2)/2 \tag{28b}$$

For numerical determination of ξ_1 and ξ_2 from Eqs. (28) in terms of $t_f/2$, it is helpful to define an amplitude A and a phase γ thus:

$$A^2 \triangleq (c \cdot ch - 1)^2 + s^2 \cdot sh^2$$
$$\gamma \triangleq \tan^{-1}(c \cdot ch - 1)/(s \cdot sh), \qquad (-\pi \le \gamma \le \pi) \tag{29}$$

Anticipating our later needs, we observe that for an undamped mode

$$\gamma = \tan^{-1}[(c-1)/0] = -\pi/2 \qquad (\text{when } \zeta_\mu = 0) \tag{30a}$$

where $(-\pi/2)$ is selected because $-2 \le (c-1) \le 0$, while for $\zeta_\mu \to 0$

$$\lim_{\zeta_\mu \to 0}: \gamma = \tan^{-1} 2(c-1)/(s\zeta_\mu \omega_\mu t_f) \tag{30b}$$

Because $(c-1)$ is negative semidefinite and $s \triangleq \sin(\omega_\mu t_f/2)$ is sign indefinite, the phase γ, depending on the sign of s, for $\zeta_\mu > 0$, is

$$\gamma \ge -\pi/2 \qquad \text{or} \qquad \gamma \le -\pi/2 \qquad (\text{when } \zeta_\mu > 0) \tag{30c}$$

For a given ω_μ, the quantity $\sin(\omega_\mu t_f/2)$ will change little with ζ_μ because t_f is a very weak function of ζ_μ, so the sign of $\sin(\omega_\mu t_f/2)$ will remain the same for a practical range of ζ_μ. The phase γ, therefore, has two possible ranges:

$$-\pi \le \gamma \le -\pi/2$$

or

$$-\pi/2 \le \gamma \le 0 \qquad (\text{when } \zeta_\mu > 0) \tag{30d}$$

Now, with the definitions (29), Eqs. (28a) and (28b) coalesce to

$$A \sin(\omega_\mu \xi_1 + \gamma) = (sh^2 - s^2)/2 = -A \sin(\omega_\mu \xi_2 - \gamma) \tag{31}$$

The unknown ξ_1 therefore will be

$$\omega_\mu \xi_1 = \sin^{-1}[(sh^2 - s^2)/2A] - \gamma \tag{32}$$

Regarding ξ_2, Eq. (31) furnishes multiple relationships of ξ_2 with ξ_1, namely,

$$\omega_\mu \xi_2 - \gamma \stackrel{?}{=} \begin{cases} -\omega_\mu \xi_1 - \gamma, & \text{or} & \text{(33a)} \\ \pi + \omega_\mu \xi_1 + \gamma, & \text{or} & \text{(33b)} \\ -\pi + \omega_\mu \xi_1 + \gamma, & \text{or} & \text{(33c)} \\ \pm 2k\pi - \omega_\mu \xi_1 - \gamma & (k = 1,2,3\ldots) & \text{(33d)} \end{cases}$$

To sift the valid relationship from the previous five choices, note that ξ_1 and ξ_2 both must be greater than zero. On this basis, Eq. (33a) is dismissed because it yields $\xi_2 = -\xi_1$. On the same grounds, the minus sign from " $\pm$ " in Eq. (33d) can be ignored, and the plus relationship can be discarded as well because even for $k = 1$ it is not a minimum-time solution compared with Eqs. (33b) and (33c). To select from these two remaining choices, we substitute in Eq. (31) $\gamma = -\pi/2$ from Eq. (30a) for $\zeta_\mu = 0$ and obtain $\xi_1 = \xi_2$. Equation (33b) reconciles with this result, whereas Eq. (33c) does not; thus we apprehend the correct relationship:

$$\omega_\mu \xi_2 = \pi + 2\gamma + \omega_\mu \xi_1 \tag{34}$$

Whether the width ξ_2 is wider or narrower than the width ξ_1 depends on which of the two ranges in Eq. (30d) the phase γ belongs to. For the undamped case, $\xi_1 = \xi_2 = \sigma t_f/2$, and Eqs. (31) lead to

$$2\sin^2(\omega_\mu \sigma t_f/4) = \sin^2(\omega_\mu t_f/4) \tag{35a}$$

or

$$\cos(\omega_\mu \sigma t_f/2) = \cos^2(\omega_\mu t_f/4) \tag{35b}$$

Singh et al.[10] developed algebraic conditions governing the widths of the intervening pulses; but because they employed optimal control approach, their conditions involve costate

variables, unknown a priori, while the conditions (35) contain the modal frequency and the slew time only.

Summary of Algorithm

The following algorithm summarizes the steps to determine the quantities ξ_1, ξ_2, and t_f. Note that these quantities do not depend on the jet modal coefficients $\chi_{\mu J}$ because the jets producing positive or negative angular accelerations are taken to be located symmetrically around the vehicle mass center and to be residing in the central body.

1) First identify the mode vulnerable to the slew maneuver. This is usually a low-frequency mode that has a significant rotational modal coefficient Φ_μ contributing to the spacecraft attitude $\theta(t)$, Eq. (6). Ascertain its frequency ω_μ and the damping coefficient ζ_μ (this ascertainment may not be a simple task, though).

2) Given the maneuver angle $(\Theta_f - \Theta_i)$, the spacecraft's central, principal moment of inertia I about the slew axis, slew torque T_{mx}, and the thrust force F_{mx};

3) Assume $\sigma_1 = 0 = \sigma_2$ and so $\xi_1 = 0 = \xi_2$ [Eqs. (15)], and determine approximate $t_f/2$ using Eq. (17c).

4) For this $t_f/2$, determine the quantities *c, s, ch, sh* [Eq. (26)] and the amplitude A and phase γ; then solve Eq. (32) for ξ_1 and Eq. (34) for ξ_2.

5) Using Eq. (15), now determine σ_1 and σ_2; substitute these new values in Eq. (17c) and evaluate an improved $t_f/2$.

6) Return to step 4 and iterate until ξ_1, ξ_2, and $t_f/2$ each converge to the true solution within desired accuracy.

In contrast to this simple iterative algorithm, Homotopy method was resorted to in Ref. 10 to solve the zero-residual-energy conditions stated therein.

IV. Numerical Results and Discussion

The preceding analysis is now illustrated on a generic spacecraft, shown in Fig. 4, whose elasticity stems from two symmetrically located flexible appendages. The modal characteristics of the spacecraft, two modes per axis, are displayed in Table 1; note in Table 1 though that mode 6 contributes to both the x and z axes. In the $(\Phi_\mu^2/\omega_\mu^2)$ column, we observe that for the spacecraft at hand the step response of the second mode for each axis is two to four orders of magnitude smaller than that of the corresponding first mode. This of course depends on the spacecraft under consideration, but for the present this column shows that one-mode analysis in the text is adequate. Moreover, it also indicates that for none of the axes does the third mode need to be considered. The last two columns of Table 1 substantiate Eq. (1). In practice, it is seldom necessary to retain in the simulation so many modes as are necessary to satisfy Eq. (1) precisely because the high-frequency modes are not excited anyway; for more discussion along these lines, see Hughes.[20] The ratio I_f/I_r in the last column reveals that the z axis is by far the most flexible, the x axis less so, and the y axis the least; between the x and y axes, nevertheless, since the y axis interacts with the lower-frequency modes and the x axis with the higher-frequency ones, the $(\Phi_\mu^2/\omega_\mu^2)$ column suggests that the y angle will have more contributions from the modes 1 and 5 than the x angle will have from the modes 4 and 6, given the same slew torque. Regardless, we illustrate the zero-residual-energy 90-deg slews about the x and the z axes, with angular accelerations α_{mx} equal to 0.003 and 0.004275 rad/s^2, respectively. We stress, though, that in a real-life situation, unless there are countervailing reasons, a structural engineer would not approve a z slew with the array plane normal to the slew plane because that will excite the low-frequency transverse vibrations easily; instead, the arrays will be turned by 90 deg about their hinges, so that they lie in the slew plane, and thereby their antisymmetric, higher-frequency, in-plane vibrations are excited little. This is indeed the rationale behind selecting the x slew for illustration. Figure 5 illustrates, for x slew, the pulse widths $\omega_4\xi_1$ and $\omega_4\xi_2$ and the slew time t_f against the damping coefficient $0 \le \zeta_4 \le 0.0118$. When $\zeta_4 = 0$, the two pulse widths are equal (60 deg or 170 ms) as anticipated. As the damping coefficient escalates, the second pulse widens, reaching a maximum of ~230 deg (650 ms) at $\zeta_4 = 0.0118$ beyond which $|(sh^2 - s^2)/2A| > 1$ and so Eq. (32) has no solution for the selected α_{mx} and $(\Theta_f - \Theta_i)$. The variation in t_f with ζ_4 is very small indeed: a total of 16 ms over the range $0 \le \zeta_\mu \le 0.0118$. Because clean jet pulses of as narrow as 20 ms are known to be producible, the jet pulses of the range 120–260 ms for the x slew are practical. Similar to Fig. 5, the plot for z slew (not shown here to conserve space) demonstrates that, for this axis,

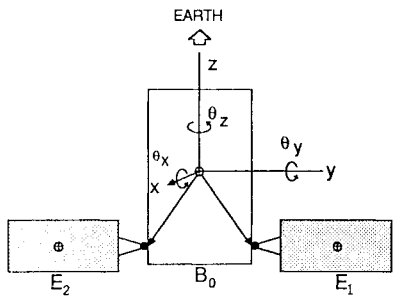

Fig. 4 Generic deformable spacecraft.

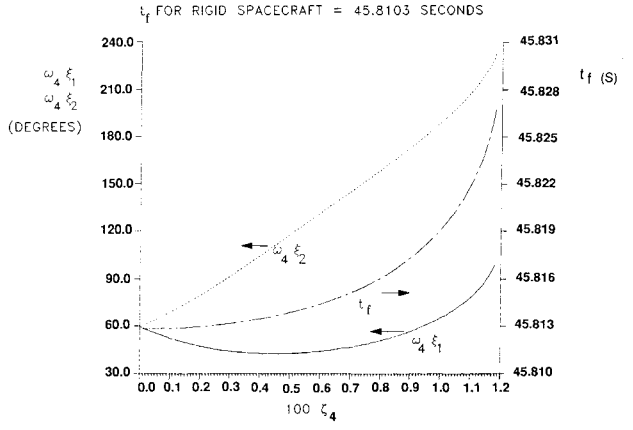

Fig. 5 x slew: two intervening pulse-widths and slew time t_f against damping coefficient ζ_4.

Table 1 Modal characteristics of the generic spacecraft in Fig. 4

Axis	Two low-frequency interacting modes	Frequency ω_μ, rad/s	Rotational modal coefficient Φ_μ	Φ_μ^2/ω_μ^2 (step response indicator)	$I\Phi_\mu^2$	$\sum_{\mu=1}^{2} I\Phi_\mu^2$	I_f/I_r
x	In-plane antisymmetric 4	6.102	−0.328 E-2	2.892 E-7	0.3836	0.3839	0.47
	bending 6	10.33	0.101 E-3	9.373 E-11	0.3560 E-3		
y	Symmetric transverse 1	1.765	−0.116 E-2	4.313 E-7	0.033	0.046	0.064
	bending 5	9.653	−0.728 E-3	5.684 E-9	0.013		
z	Antisymmetric 2	2.53	−0.866 E-2	1.172 E-5	1.186	1.584	1.703
	transverse bending 6	10.33	−0.502 E-2	2.36 E-7	0.398		

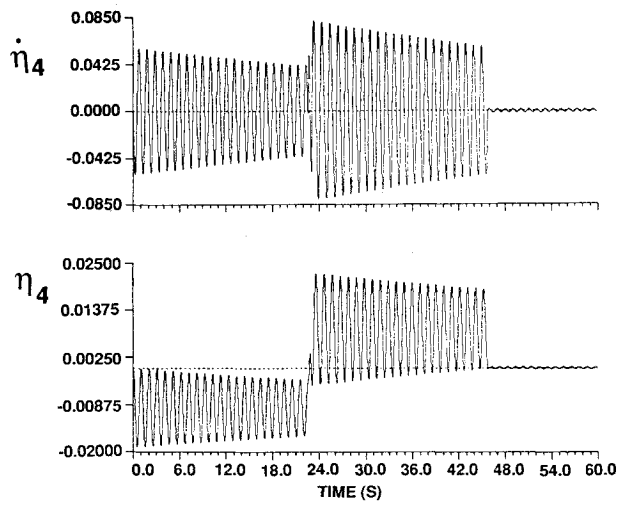

Fig. 6 x slew: modal coordinate η_4 and its rate $\dot{\eta}_4$ when $\zeta_4 = 0.0025$ and the zero-residual-energy torque profile is also based on $\zeta_4 = 0.0025$.

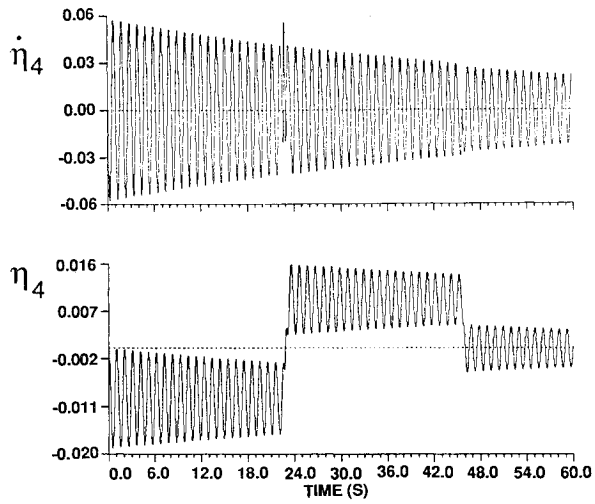

Fig. 7 x slew: modal coordinate η_4 and its rate $\dot{\eta}_4$ when $\zeta_4 = 0.0025$ and the zero-residual-energy torque profile is based on $\zeta_4 = 0.0$.

the width $\omega_2\xi_1$ is wider than $\omega_2\xi_2$. Thus the two slews are examples of the two possible ranges of γ shown in Eq. (30d).

Next, Fig. 6 illustrates the excitation of mode 4 when the x slew takes place with a zero-residual-energy torque profile, with $\zeta_4 = 0.0025$. The modal amplitude envelopes of η_4 are exactly as depicted in Fig. 3, and after the slew the energy in mode 4 is indeed miniscule (theoretically, zero), as intended. Figure 7, on the other hand, illustrates the residual excitation of mode 4 if the x slew takes place with a three-switch torque profile based on zero damping while the mode does have damping equal to $\zeta_4 = 0.0025$. A careful observation reveals that when the slew ends, $\dot{\eta}_4$ is zero; only η_4 is nonzero due to the structural damping. Spacecraft attitude oscillations, due to the residual modal amplitudes in Figs. 6 and 7, are displayed in the third and the second row, respectively, in Table 2. The first row in Table 2, on the other hand, furnishes the residual attitude error (theoretically zero) when there is no structural damping and the three-switch torque profile is also based on no-damping assumption (the problem studied by Singh et al.[10]). Finally, the last column and the last row in Table 2 show three- to fifty-fold increases in the residual attitude error if the conventional bang-bang torque profile is used instead of the profile with intervening pulses. The 90-deg slew per se is shown later for the case of the z slew.

Figures 8–10 pertain to the zero-residual-energy, 90-deg z slew. Figure 8 portrays different phases of excitation of mode 2 during the slew and the zero-residual-energy denouement as the slew is completed; note, in particular, how the phase at $t = t_1$ is brought to that at $t = t_3$ by switching the torque directions at t_1, t_2, and t_3, and how the phase reaches the origin at $t = t_f$ in a deadbeat fashion, as planned. It is illuminating to compare this phase plane depiction with the trajectory 0ABC0DEF0 in Fig. 1, which is applicable to an undamped mode with one-switch torque profile with the half-slew time equal to an integer times the modal period. Figure 9 illustrates the contributions of mode 2 and mode 6 separately to the z-attitude angle—0.1 deg by mode 2 and 0.002 deg by mode 6, a ratio of 50:1; this is precisely the ratio between Φ_μ^2/ω_μ^2 for $\mu = 2$ and 6 for the z axis in Table 1, and it justifies ignoring the second mode in the analysis. Also, we observe that whereas mode 2 has no residual oscillations, mode 6 does, approximately equal to 0.001 deg. Last, the phase plane of the rest-to-rest z slew with the two intervening pulses is rendered

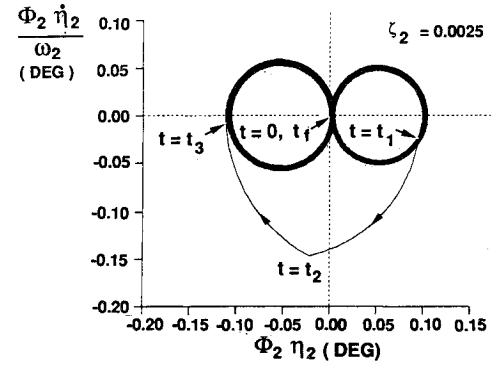

Fig. 8 z slew: mode 2 phase plane with zero-residual-energy slew.

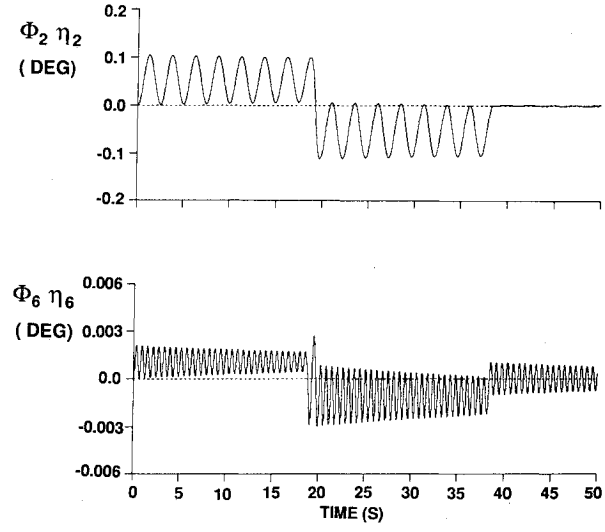

Fig. 9 z slew: attitude angles contributed by mode 2 and mode 6 vs time with zero residual energy in mode 2.

Table 2 x slew: amplitudes of residual attitude oscillations due to mode 4 ($t \geq t_f$) under four different circumstances

Mode 4 damping coefficient, ζ_4	ζ_4 for which the widths of the intervening pulses are calculated	Attitude amplitude at $t = t_f$, rad	(Residual amplitude)/(residual amplitude with bang-bang torque profile)
0.00	0.0	1.30 E-6	0.029
0.0025	0.0	1.44 E-5	0.325
0.0025	0.0025	8.20 E-7	0.0185
0.0025	——[a]	4.43 E-5	1.000

[a]No intervening purses; rigid, bang-bang torque profile.

in Fig. 10; Fig. 10a illustrates the rigid-plus flexible motion whereas Fig. 10b illustrates only the rigid motion.

V. Simultaneous, Discrete, Reaction Jet Control of One Rigid and One Elastic Mode from an Arbitrary State: Concept

We will now discuss the attitude control of a flexible spacecraft from an arbitrary state (that is, arbitrary rigid attitude and rate and arbitrary phase of one elastic mode) to the origin using reaction jets. The weighted time-fuel approaches by Vander Velde and He[6] and de Oliveira e Souza[7] do not perform satisfactorily near the origin because Ref. 6 considered

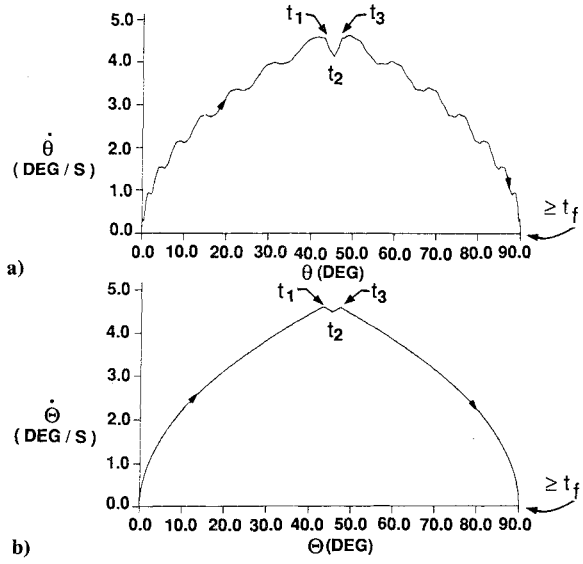

Fig. 10 z slew: a) total rate ($\dot{\theta}$) vs total angle (θ), and b) rigid rate ($\dot{\Theta}$) vs rigid angle (Θ).

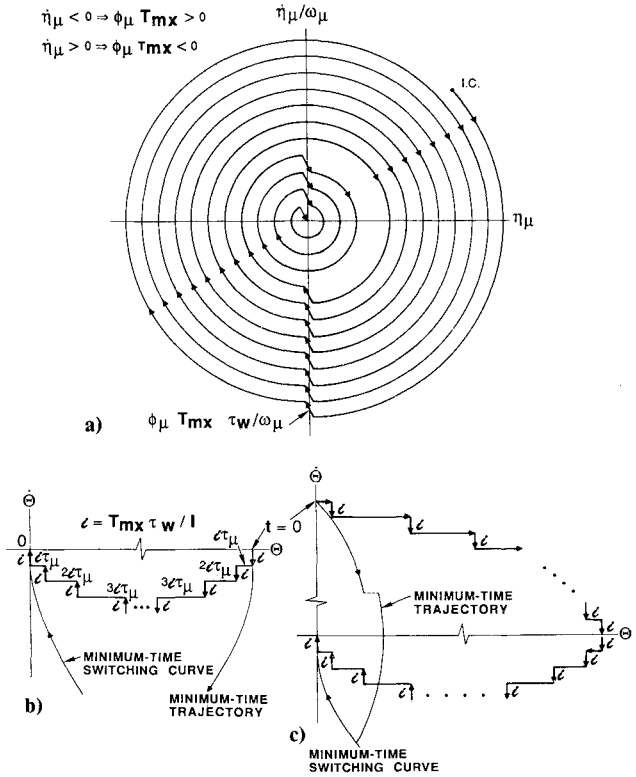

Fig. 11 Simultaneous, discrete, periodic reaction jet control of one rigid mode and one elastic mode from an arbitrary state: a) arbitrary modal state, b) arbitrary rigid angle error, and c) arbitrary rigid attitude rate error.

the rigid and the elastic mode control problems separately, and Ref. 7 determined an exact weighted time-fuel optimal solution for an elastic mode only, ignoring the rigid mode. Inasmuch as their design suffers from a dissonance between the two controllers, the unsatisfactory performance near the origin is expected. The noted discord arises because the weighted time-fuel optimal controller for a rigid mode dictates two relatively wide pulses, one in the beginning and one near the origin, whereas that for an elastic mode suggests a large number of narrow pulses, fired periodically, around the peak modal rates; this fundamental difference arises because a rigid mode has zero frequency (it has no restoring ability) whereas an elastic mode has a nonzero frequency (it has strain energy). To devise a controller that controls both a rigid mode and an elastic mode in unison, narrow pulses are desired because 1) the energy of an elastic mode diminishes more rapidly with the jet firings around the peak modal rates, and 2) the undesirable excitation of the high-frequency modes, proportional to the pulsewidth, then becomes less annoying. Of course, in the process, the rigid mode control might lengthen in time. One such discrete controller is shown schematically in Fig. 11. Figure 11a portrays discretely diminishing amplitude of an elastic mode due to the narrow jet pulse firings, initially around the negative peak modal rates. Treating the jet pulse $\tau_w s$ long (usually 20–80 ms) as an impulse of the linear momentum $F_{mx}\tau_w$ or, equivalently, the angular momentum $T_{mx}\tau_w$, Ref. 5 shows that this impulse decreases the modal energy by $\Delta E_\mu = \chi_{\mu J} F_{mx}\tau_w \dot{\eta}_\mu$ where $\dot{\eta}_\mu$ is the modal rate just before the firing. To insure that $\Delta E_\mu < 0$, the direction of the force F_{mx}, the modal displacement $\chi_{\mu J}$ at the jet location, and the modal rate $\dot{\eta}_\mu$ all must be such that $\chi_{\mu J} F_{mx}\dot{\eta}_\mu < 0$ and if $\dot{\eta}_\mu < 0$, as in Fig. 11a for the first set of pulses, then $\chi_{\mu J} F_{mx} > 0$, or equivalently, $\Phi_\mu T_{mx} > 0$. With this ΔE_μ, and knowing that $\eta_\mu \simeq 0$ at the time of the firing, one can show that the instantaneous change in the modal rate is $-|\chi_{\mu J} F_{mx}|\tau_w$ [shown in Fig. 11a, after invoking Eq. (4)] and the change in the modal amplitude is $-|\chi_{\mu J} F_{mx}|\tau_w/\omega_\mu$. In Fig. 11a, the firings are shown to be of finite but small pulse width, to incorporate the reality that they are so. To determine an optimum pulse width, both the elastic and the rigid mode must be considered. Now, the angular momentum impulse $T_{mx}\tau_w$ produces an instantaneous change in the attitude rate equal to $T_{mx}\tau_w/I \triangleq \epsilon$, and the repetitive periodic pulses (of the period τ_μ) bring a succession of change in the angular rate and position of the spacecraft. For instance, the initial positive attitude and positive rate shown in Figs. 11b and 11c, respectively, at $t = 0$, dictate that for some initial pulses the attitude rate change ϵ must be $\epsilon < 0$, and so T_{mx} must be $T_{mx} < 0$; later on, the torque T_{mx} and the rate change ϵ must reverse their signs. The transition from $T_{mx} < 0$ to $T_{mx} > 0$, or vice versa for other initial conditions, takes place in half modal period, as shown in Fig. 11a. Note that whereas T_{mx} changes its sign (just for once, as in the weighted time-fuel optimal control problem) to bring the rigid state to zero, the elastic mode control must also switch to the other peak modal rate to ensure that ΔE_μ remains less than zero. (For the thrusters located on the central rigid body, the modal rotation Φ_μ is independent of their location.) Returning to the determination of an optimal pulsewidth τ_w, it may now be clear that τ_w must be such that both the rigid and the elastic modes are brought down to zero simultaneously; the analysis to this effect is not within the scope of this paper. In Figs. 11b and 11c, the present discrete controller is compared with the minimum-time rigid body controller. Since the former controller controls both modes, it is necessarily slower than the latter. Also, the angles $i\tau_\mu, 2i\tau_\mu, \ldots$, shown in Fig. 11b are the angles traveled by the spacecraft during different τ_μ periods between two successive jet firings.

VI. Concluding Remarks

Engineering realization of the torque profile with two intervening pulses, to effect a zero-residual-energy slew, depends on the precision with which the critical modal frequency and

damping are known. When the frequency is not known accurately (the usual case), it may be determined with adequate accuracy during the first segment of the slew by passing the attitude signal through a bandpass filter, provided the filter's rise time t_r is less than the half-slew time $t_f/2$. If B is the bandwidth of the filter, then t_r is governed by $t_r B = 2\pi$. Moreover, if $t_f/2$ spans many modal periods, then t_r can be set to be equal to, say, five periods, but still shorter than $t_f/2$, and the bandwidth B in turn becomes one-fifth of the modal frequency. This helps in rejecting the neighboring modes, in reducing the overshoot, and in settling over the modal wave of interest, which then yields an accurate, timely knowledge of the modal frequency. With regard to the structural damping, this too could be determined by observing the slow amplitude decay of the extracted modal wave, provided the half-slew time is sufficiently long; otherwise, different techniques are called for—perhaps an in-flight active excitation experiment with thrusters before the slew. In the preceding analysis, it is assumed that the thrusters produce equal positive and negative torques; when this is not so, the analysis must be modified. Last, the symmetry of the modal rate history and antisymmetry of the modal coordinate history of an undamped mode with respect to the half slew time—of importance in the optimal control approach for simplifying the algebra—is of no significance in the dynamics approach adopted here.

References

[1]Athans, M., and Falb, P. L., *Optimal Control: An Introduction to the Theory and Its Applications*, McGraw-Hill, New York, 1966, Secs. 7.2 and 8.4–8.8.

[2]D'Amario, L. A., and Stubbs, G. S., "A New Single-Rotation Axis Autopilot for Rapid Spacecraft Attitude Maneuvers," *Journal of Guidance and Control*, Vol. 2, No. 4, 1979, pp. 339–346.

[3]Farrenkopf, R. L., Sabroff, A. E., and Wheeler, P. C., "Integral Pulse Frequency On-Off Control," *Guidance and Control—II*, edited by R. C. Langford and C. J. Mundo, Progress in Astronautics and Aeronautics, Vol. 13, AIAA, New York, 1964, pp. 185–230.

[4]White, L. R., Colburn, B. K., and Boland, J. S., III, "Design Analogy between Optimal Time-Fuel and Rate-ledge Relay Controllers," *Journal of Spacecraft and Rockets*, Vol. 13, No. 4, 1976, pp. 214–219.

[5]Hablani, H. B., and Jansz, J., "Self-Balanced Active Modal Damping for Flexible Spacecraft Using Thrusters and Bandpass Filters," *Proceedings of the AIAA Guidance, Navigation, and Control Conference*, AIAA Paper 89-3536, AIAA, Washington, DC, 1989, pp. 949–963.

[6]Vander Velde, W. E., and He, J., "Design of Space Structure Control Systems Using On-Off Thrusters," *Journal of Guidance, Control, and Dynamics*, Vol. 6, No. 1, 1983, pp. 53–60.

[7]De Oliveira e Souza, M. L., "Exactly Solving the Weighted Time/Fuel Optimal Control of an Undamped Harmonic Oscillator," *Journal of Guidance, Control, and Dynamics*, Vol. 11, No. 6, 1988, pp. 488–494.

[8]Skaar, S. B., Tang, L., and Yalda-Mooshabad, I., "On-Off Attitude Control of Flexible Satellites," *Journal of Guidance, Control, and Dynamics*, Vol. 9, No. 4, 1986, pp. 507–510.

[9]Rajan, N., "Minimum Time Slewing of the SIRTF Spacecraft," *Proceedings of the AIAA Guidance, Navigation, and Control Conference*, Vol. 2, AIAA Paper 87-2527, AIAA, Washington, DC, 1987, pp. 1222–1228.

[10]Singh, G., Kabamba, P. T., and McClamroch, N. H., "Planar, Time-Optimal, Rest-to-Rest Slewing Maneuvers of Flexible Spacecraft," *Journal of Guidance, Control, and Dynamics*, Vol. 12, No. 1, 1989, pp. 71–81.

[11]Junkins, J. L., and Turner, J. D., *Optimal Spacecraft Rotational Maneuvers*, Elsevier Science Publishers, New York, 1986.

[12]Breakwell, J. A., "Optimal Feedback Slewing of Flexible Spacecraft," *Journal of Guidance and Control*, Vol. 4, No. 5, 1981, pp. 472–479.

[13]Juang, J.-N., Horta, L. G., and Robertshaw, H. H., "A Slewing Control Experiment for Flexible Structure," *Journal of Guidance, Control, and Dynamics*, Vol. 9, No. 5, 1986, pp. 599–607.

[14]Junkins, J. L., Rahman, Z., and Bang, H., "Near-Minimum-Time Control of Distributed Parameters: Analytical and Experimental Results," *Journal of Guidance, Control, and Dynamics*, Vol. 14, No. 2, 1991, pp. 406–415.

[15]Byers, R. M., Vadali, S. R., and Junkins, J. L., "Near-Minimum Time, Closed-Loop Slewing of Flexible Spacecraft," *Journal of Guidance, Control, and Dynamics*, Vol. 13, No. 1, 1990, pp. 57–65.

[16]Hughes, P. C., and Abdel-Rahman, T. M., "Stability of Proportional-Plus-Derivative-Plus Integral Control of Flexible Spacecraft," *Journal of Guidance and Control*, Vol. 2, No. 6, 1979, pp. 499–503.

[17]Hablani, H. B., "Constrained and Unconstrained Modes: Some Modeling Aspects of Flexible Spacecraft," *Journal of Guidance and Control*, Vol. 5, No. 2, 1982, pp. 164–173.

[18]Hughes, P. C., "Modal Identities for Elastic Bodies, with Application to Vehicle Dynamics and Control," *Journal of Applied Mechanics*, Vol. 47, No. 1, 1980, pp. 177–184.

[19]Bisplinghoff, R. L., Ashley, H., and Halfman, R. L., *Aeroelasticity*, Addison-Wesley, Reading, MA, 1955.

[20]Hughes, P. C., "Space Structure Vibration Modes: How Many Exist? Which Ones Are Important?" *Proceedings of the Workshop on Applications of Distributed System Theory to the Control of Large Space Structures*, Jet Propulsion Lab., California Inst. of Technology, JPL Pub. 83-46, Pasadena, CA, 1983, pp. 31–47.